Mitochondrial p53 mediates a transcription-independent regulation of cell respiration and interacts with the mitochondrial F F -ATP synthase

Marie Bergeaud, Lise Mathieu, Arnaud Guillaume, Ute M. Moll, Bernard Mignotte, Nathalie Le Floc'H, Jean-Luc Vayssière, Vincent Rincheval, Nathalie Le Floch

Title: **Mitochondrial p53 mediates a transcription-independent regulation of cell respiration and interacts with the mitochondrial F_1F_0-ATP synthase**

Marie Bergeaud [1,†], Lise Mathieu [1,†], Arnaud Guillaume [1], Ute M. Moll [2], Bernard Mignotte [1], Nathalie Le Floch [1], Jean-Luc Vayssière [1] and Vincent Rincheval [1,*]

[1] Laboratoire de génétique et biologie cellulaire (LGBC), Université de Versailles St Quentin-en-Yvelines / Ecole Pratique des Hautes Etudes, EA4589, UFR des Sciences de la santé, 2 avenue de la source de la Bièvre, 78180 Montigny-le-Bretonneux, France

[2] Department of Pathology, Stony Brook University, Stony Brook, NY 11794, USA

* Corresponding author. Address: Université de Versailles St Quentin-en-Yvelines, Laboratoire EPIM, EA3647, UFR des Sciences de la Santé, 2 avenue de la source de la Bièvre, 78180 Montigny-le-Bretonneux, France.

Tel: (+33) 1 70 42 93 57

E-mail address: vincent.rincheval@uvsq.fr

† These authors contributed equally to this work.

Keywords: Tumor suppressor, p53, cancer, mitochondria, energetic metabolism, oxidative phosphorylation, respiration, OSCP, reactive oxygen species.

Abstract:

We and others previously reported that endogenous p53 can be located at mitochondria in the absence of stress, suggesting that p53 has a role in the normal physiology of this organelle. The aim of this study was to characterize in unstressed cells the intramitochondrial localization of p53 and identify new partners and functions of p53 in mitochondria. We find that the intramitochondrial pool of p53 is located in the intermembrane space and the matrix. Of note, unstressed HCT116 $p53^{+/+}$ cells simultaneously show increased O_2 consumption and decreased mitochondrial superoxide production compared to their p53 null counterpart. This data was confirmed by stable H1299 cell lines expressing low levels of p53 specifically targeted to the matrix. Using immunoprecipitation and mass spectrometry, we identified the Oligomycin Sensitivity-Conferring Protein (OSCP), a subunit of the F_1F_0-ATP synthase complex, as a new partner of endogenous p53, specifically interacting with p53 localized in the matrix. Interestingly, this interaction seems implicated in mitochondrial p53 localization. Moreover, p53 localized in the matrix promotes the assembly of F_1F_0-ATP synthase. Taking into account that deregulations of mitochondrial respiration and reactive oxygen species production are tightly linked to cancer development, we suggest that mitochondrial p53 may be an important regulator of normal mitochondrial and cellular physiology, potentially exerting tumor suppression activity inside mitochondria.

Abbreviations: IMS: inner membrane space; OSCP: oligomycin sensitivity-conferring protein; ROS: reactive oxygen species.

Introduction

The human p53 protein is encoded by the *TP53* gene which is mutated in approximately 50% of human cancers, representing the most common genetic lesion associated with this type of disease.[1] It is well known that the p53 protein is a transcription factor [2-5] harbouring low basal levels which can rapidly be activated and stabilized in response to multiple stresses.[6, 7] Hundreds of p53-regulated genes have now been discovered which participate in many biological processes such as cell cycle, senescence, apoptosis, metabolism, and DNA repair,[8-10] suggesting that the main functions of p53 might be executed by its nuclear transcriptional activities. Many efforts have been devoted to study p53-mediated apoptosis and senescence since these processes are still presumed to be particularly important for p53's tumor suppressor activity.[11]

More than a decade ago, it was shown that p53 can also promote apoptosis in a transcription-independent manner, although its mechanism was unknown.[12-18] Subsequently it was observed that in response to stress, a fraction of p53 rapidly localizes to mitochondria, prior to p53 nuclear accumulation, triggering mitochondrial outer membrane permeabilization and caspase activation.[19-22] It was demonstrated that targeting p53 specifically to mitochondria *via* fusion with import leader peptides is sufficient to induce apoptosis in p53-deficient cells.[19] When accumulating at mitochondria, p53 is able to trigger apoptosis through its dual capacity of derepressing as well as directly activating several pro-apoptotic members of the Bcl-2 family at the outer membrane.[23-25] These activities respectively depend on the ability of p53 to dissociate anti-apoptotic Bcl-xL, Bcl-2 and Mcl-1 from their pro-apoptotic partners Bax, Bak and tBid or to directly activate Bak and Bax (reviewed in Vaseva [26]). Several studies have reported that the DNA binding domain of p53 is also important in its mitochondrial roles of Bcl-2 family de-repressor and activator.[20, 27-30]

On the other hand, it is now becoming obvious that some p53 functions occur in the absence of acute stress. These p53 functions depend on basal levels of p53 or the activation of p53 by low levels of constitutive stress.[31] Several studies have indicated that p53 can

participate in the regulation of metabolism,[32] for instance by inducing transcription of the nuclear gene encoding the SCO2 protein, which is critical for regulating the mitochondrial cytochrome c oxidase (COX) respiratory chain complex.[33] Changes in metabolic regulations are important in the development of cancers. The Warburg effect describes the seemingly paradoxical fact that despite sufficient oxygen availability, most cancer cells predominantly produce energy by a high rate of (low yielding) glycolysis rather than by (high yielding) oxidative phosphorylation.[34] Interestingly, p53 can inhibit glycolysis by decreasing the expression of several glucose transporters.[35, 36] The p53-dependent induction of the *TIGAR* gene also triggers an inhibition of glycolysis *via* a decrease in fructose-2,6-biphosphate levels.[37] Furthermore, basal levels of p53 were shown to diminish reactive oxygen species (ROS) levels within the cell by inducing the expression of detoxifying enzymes such as GPX,[38-40] MnSOD,[39] catalase in certain cell types [41] and sestrins.[42, 43] Paradoxically, p53 has also been described to upregulate the expression of pro-oxidant factors such as PIG3,[44] PIG6 [45] or FDXR [46] and to repress expression of MnSOD during acute stress.[47] This complex situation has led to the postulate that p53 could assume the role of a protector or a killer, depending on the type and severity of stress.

As previously observed in studies focusing on p53 apoptotic functions, it has been shown that p53 can also regulate normal mitochondrial physiology through transcription-independent activities. Several studies, performed with cells that either overexpress or lack p53 have shown that p53 can interact with mitochondrial proteins located in the mitochondrial matrix, such as the DNA polymerase γ which is involved in the synthesis and repair of mtDNA. This interaction could account for a higher mtDNA copy number in $p53^{+/+}$ *versus* $p53^{-/-}$ cells.[48-52]

We and others have previously characterized that endogenous p53 can be located at mitochondria in the absence of exogenous stress, further supporting that p53 has a role in the normal physiology of this organelle.[53-55] In the present study, our aim was to better

characterize the intramitochondrial localization of p53 and to identify new partners and functions of p53 in mitochondria in the absence of induced stress. Here we established that most of the intramitochondrial pool of p53 is present in the two soluble compartments of mitochondria, with higher amounts of p53 in the intermembrane space (IMS) than in the matrix. Using the human lung carcinoma H1299 cell line specifically expressing mitochondrially targeted p53 in the IMS (H1299-p53-IMS) or in the matrix (H1299-p53-Mx), we have observed that addressing low levels of p53 to the matrix is sufficient to simultaneously increase oxygen consumption and decrease mitochondrial superoxide production. By immunoprecipitation and mass spectrometry approaches, we also identified the Oligomycin Sensitivity-Conferring Protein (OSCP), a component of the F_1F_0-ATP synthase, as a new partner of endogenous mitochondrial p53, specifically interacting with p53 localized in the matrix. Interestingly, we have observed that this interaction could be implicated in mitochondrial localization of p53. We have also shown that p53 localized in the matrix promotes the assembly of the F_1F_0-ATP synthase complex. In conclusion, our results demonstrate that in the absence of stress, low levels of mitochondrial p53 can have important effects on mitochondrial physiology, notably on cell respiration. Considering the importance of such processes in the development of several pathologies such as cancer, we suggest that mitochondrial p53 could be an important regulator of normal mitochondrial and cellular physiology, potentially exerting tumor suppression activities inside mitochondria.

Materials and Methods

Construction of cell lines stably expressing mitochondrially targeted p53. The p53-Mx vector allowing the expression of p53 to the mitochondrial matrix was constructed by Pr. Ute M. Moll's laboratory.[19] In this pcDNA3 derived vector, the sequence encoding mitochondrial import leader of ornithin transcarbamylase is fused to the N-terminus of human wild type p53 coding sequence. The p53-IMS vector was used to address p53 to the mitochondrial intermembrane space. This vector was derived from the pIRES-cytb2-WTSOD1 plasmid that was kindly given by Dr. Jordi Magrané, *Weill Medical College of Cornell University, USA*.[56] Briefly, the WTSOD1 coding sequence was replaced with the human wild type p53 coding sequence. The WTSOD1 sequence was removed by enzymatic cleavage with NotI and BstXI. The p53 sequence was PCR-amplified using primers displaying NotI (forward primer) or BstXI (reverse primer) restriction sites. The PCR product was then subcloned into pJET1.2 vector (CloneJet PCR cloning kit, Fermentas) to facilitate the cleavage by the appropriate restriction enzymes. The digestion product was cloned in frame with the C-terminus of the mitochondrial targeting sequence plus four amino acids of CytB2. The p53-IMS vector construction was verified by sequencing (Eurofins MWG Operon). For establishment of cell lines, H1299 p53-null cells were plated in 60 mm diameter Petri dishes, transfected with 10 µg of the p53-IMS vector, p53-Mx vector or pcDNA3 plasmid as control, using lipofectamin 2000 (Invitrogen) at 80% confluence and transferred in two 100 mm diameter Petri dishes 24 hours post-transfection. Transfected cells were then selected under G418 treatment and individual clones were isolated after 2 weeks of selection.

Cell lines and cell culture. HCT116 human colorectal carcinoma cells $p53^{+/+}$ and $p53^{-/-}$,[57] H1299 human lung adenocarcinoma cells (p53 null) and its derivatives (p53-Mx, p53-IMS and pcDNA3), were grown in DMEM F-12 medium (Invitrogen) supplemented with 10% fetal bovine serum, 1% Glutamax (v/v), 100 µg/ml penicillin and 100 U/ml streptomycin, at

37°C in a humidified atmosphere containing 5% CO_2. In order to induce genotoxic stress, cells were treated with 125 µg/ml etoposide (Sigma Aldrich) for 24 hours.

siRNA transfection. To inhibit OSCP expression, 7.10^5 HCT116 cells were seeded in 60 mm cell culture dishes. 24 hours later, cells were transiently transfected with lipofectamine 2000 (Invitrogen) according to the manufacturer's instructions, with a mix containing 11 µl of Lipofectamine 2000 reagent (Invitrogen) and 162 nM of siRNA oligonucleotides for OSCP (sc-62452, Santa Cruz Biotechnology) or 162 nM of control siRNA (sc-37007, Santa Cruz Biotechnology). 72 hours following transfection, cells were collected for cell fractionation with Qproteome Mitochondria Isolation kit (Qiagen).

Cell fractionation and mitochondria isolation. Mitochondria from HCT116 and H1299 cells have been prepared using (1) the Qproteome mitochondria isolation kit (Qiagen) or (2) a conventional differential centrifugation procedure [58] for preparation of large amounts of mitochondrial fractions. (1) Briefly, cells were harvested, washed in 0,9% NaCl and incubated for 10 min at 4°C in lysis buffer. The homogenate was centrifuged at 1000 g for 10 min at 4°C, the supernatant was designated as cytosolic fraction. The pellet was resuspended in disruption buffer, passed through a 26-gauge needle 15 times. Enriched nuclei fraction was pelleted by centrifugation at 1000 g during 10 min and was homogenized in disruption buffer. To obtain the enriched mitochondrial fraction, the supernatant was centrifuged at 6000 g for 10 min at 4°C and resuspended in mitochondria storage buffer. All buffers except mitochondria storage buffer were supplemented with protease inhibitors at 1:100, provided within the kit. Protein concentration of the different fractions was determined with the BCA protein assay kit (Pierce). (2) Cell pellets were resuspended in fractionation buffer A (250 mM sucrose, 0,1 mM EDTA, 1 mM EGTA, 10 mM Hepes-KOH pH 7,4) and incubated 30 min at 4°C. Cell disruption was performed by passing the cells through a 26-gauge needle 10-15 times. The homogenates were centrifuged at 700 g for 10 min at 4°C. The supernatants

were removed and centrifuged at 7000 g for 20 min at 4°C. The mitochondria pellets were washed in fractionation buffer B (250 mM sucrose, 5 mM succinate, 5 mM KH_2PO_4, 10 mM Hepes-KOH pH 7,4). All buffers were supplemented with 1mM protease inhibitors (Aebsf, Roche).

Mitochondrial subfractionation. For subfractionation, mitochondria were harvested using the Qproteome mitochondria isolation kit (Qiagen) and washed in isotonic buffer (250 mM sucrose, 10 mM Tris-HCl) by centrifugation at 14000 g for 10 min at 4°C to discard mitochondria storage buffer (Qiagen). Mitochondria pellets were resuspended in 10 mM Tris-HCl buffer with or without 250 mM sucrose. Mitochondria or mitoplasts were respectively obtained and treated with increasing quantities of proteinase K (150 ng, 300 ng and 450 ng per 50 µg of mitochondrial proteins) and incubated on ice for 45 min. Proteinase K was finally inactivated by adding the protease inhibitor PMSF at 1mM. Treated samples were resuspended in a 250 mM sucrose, 10 mM Tris-HCl, 90 mM KCl buffer supplemented with PMSF at 1mM and immediately loaded onto NuPAGE 4-12% Bis Tris polyacrylamide gels (Invitrogen) for western blot analysis.

Immunoprecipitation and Mass Spectrometry. Mitochondrial pellets, isolated by a conventional differential centrifugation procedure,[58] were lysed in 1% digitonin buffer (150 mM NaCl, 5 mM EDTA, 1% digitonin, 50 mM Tris-HCl pH7,5) for 1 hour. p53 was immunoprecipitated from 250 µg of mitochondrial lysate with anti-p53 agarose conjugated beads (FL-393; sc-6243 AC, Santa Cruz Biotechnology) or with control IgG agarose conjugated beads (normal rabbit IgG-AC; sc-2345, Santa Cruz Biotechnology) at 4°C overnight. Samples were next washed 5 times with 0,5% digitonin buffer (150 mM NaCl, 5 mM EDTA, 0,5% digitonin, 50 mM Tris-HCl pH7,5). All buffers were supplemented with 1mM protease inhibitors (Aebsf, Roche). The immunoprecipitated proteins were eluted, loaded onto NuPAGE 4-12% Bis Tris polyacrylamide gels (Invitrogen) and analyzed by

immunoblotting or stained with Coomassie Blue (Bio-Safe Coomassie Stain, BIO-RAD) for 1 hour and rinsed in ultrapure H_2O for LC-MS/MS analyses. After staining, spots corresponding to immunoglobulin were eliminated. The remaining gel was treated, proteins isolated and digested with trypsin prior to analysis by an LTQ Orbitrap mass spectrometer, at mass spectrometry facility PAPPSO (Dr A. Guillot, INRA Jouy-en-Josas, France).

SDS-PAGE electrophoresis and Western blot. Protein samples were resolved by NuPAGE 4-12% Bis Tris polyacrylamide gels (Invitrogen) and transferred to polyvinylidene difluoride membranes (Millipore). Membranes were blocked with 5% nonfat milk in TBS-Tween (25 mM Tris-HCl pH 7,6, 150 mM NaCl, 0,1 % Tween 20) for 1 hour at room temperature and incubated with primary antibody for 2 hours at room temperature or overnight at 4°C. The following primary antibodies were used: anti-p53 (DO-1, sc-126, Santa Cruz Biotechnology) 1:500, anti-PCNA (Sigma Aldrich) 1:500, anti-enolase (gift from N. Lamande, College de France) 1:500, anti-VDAC1 (31HL Ab-1, Calbiochem) 1:1000, anti-OSCP (ATP5O, Mitosciences) 1:1000, anti-mitofilin (PA1-16918, Pierce antibodies) 1:2000, anti-Tom40 (H300, sc-11414, Santa Cruz Biotechnology) 1:500, anti-actin (Sigma Aldrich) 1:200, anti-Bak (G23, sc-832, Santa Cruz Biotechnology) 1:500, anti-lamin A/C (Cell Signaling) 1:1000, anti-MnSOD (Millipore) 1:500. After washing with TBS-Tween 0.1% (v/v), immunoblots were incubated with horseradish peroxidase-conjugated secondary antibodies (Jackson ImmunoResearch) 1:10000, for 1 hour. Proteins on the membranes were detected by immobilon chemiluminescent HRP Substrate (Millipore), visualized and quantified using ChemiDoc XRS+ system (BIO-RAD).

Analysis of F_1F_0-ATP synthase complex assembly by blue native gel electrophoresis (BN-PAGE). Mitochondria prepared using the Qproteome mitochondria isolation kit were resuspended in PBS supplemented with 1 mM protease inhibitors (Aebsf, Roche). Mitochondrial complexes were solubilized in Native Page Sample Buffer (Invitrogen),

supplemented with digitonin (1%) and centrifuged at 20000 g for 30 min at 4°C. The Native Page G-250 Sample Additive (0,1%) was added to samples just before loading onto Blue-Native Page 3-12% polyacrylamide gels (Invitrogen).

Oxygen consumption measurement. Cells were harvested, centrifuged and resuspended in DMEM F-12 lacking Glutamax, supplemented with 10% Fetal Bovine Serum. Oxygen consumption was measured using a Clark electrode at 37°C. 1.10^7 cells were transferred in 900 µl of the equilibrated medium into the oxygraphic chamber to record the endogenous oxygen concentration. Rate of oxygen consumption was determined by calculating the linear slope of oxygen concentration in nanomoles of O_2 per milliliters per minute.

ROS measurement. MitoSOX (Invitrogen) was used to measure the mitochondrial production of superoxide. The MitoSOX reagent is live-cell permeant and is rapidly and selectively targeted to the mitochondria. Once in the mitochondria, MitoSOX Red is oxidized by superoxide and exhibits red fluorescence. Briefly, cells were trypsinized, centrifugated and pellets were resuspended at 1.10^5 cells / ml in culture medium. 5 µM MitoSOX were added to the cells placed at 37°C. Red fluorescence was then measured by flow cytometry each 10 min by analyzing 2000 events per experimental condition, during at least 1 hour, in order to check the linearity of fluorescence evolution. The increase of MitoSOX fluorescence (arbitrary unit) / min was then calculated for each condition. Controls using the uncoupling agent mClCCP (250 µM) and the electron transport chain inhibitor NaN_3 (10 mM) were performed to check the specificity of the reaction: mClCCP and NaN_3 respectively increase and inhibit mitochondrial superoxide production and generation of MitoSOX red fluorescence (not shown). Flow cytometric measurements were performed using a XL3C flow cytometer (Beckman-Coulter). Fluorescence was induced by the blue line of an argon ion laser (488 nm) at 15 mW. Red fluorescence was collected with a 620 nm band pass filter.

Statistical analyses. To compare two groups Student t-test was used. $p < 0.05$ was accepted as significant. Probabilities values were indicated in the figures.

Results

p53 localizes at mitochondria in the intermembrane space and matrix compartments in HCT116 unstressed cells. p53 localization in stress conditions has been intensively studied and it was observed that p53 accumulates in nucleus and in mitochondria after stress induction. Without stress induction, the endogenous level of p53 is low and its functions remain to be precisely identified. In this condition, we previously reported that p53 can localize at mitochondria in human and rodent proliferative cells.[54] Here we attempted to verify if this phenomenon is general. To this end, we tested if basal p53 is located at mitochondria in other cell lines, including human colorectal carcinoma HCT116 cells expressing wild type p53. Cells were also cultivated with etoposide for 24 hours, a treatment used as control for stress condition. Etoposide is a topoisomerase II inhibitor that induces to single-strand and double-strand DNA breaks.[59] These damages cause post-translational modifications and stabilization of p53, which accumulates in nucleus and mitochondria. In both conditions (+/- etoposide), we examined p53 localization by cell fractionation (**Fig. 1A**, left panel). The reliability of fractionation experiments was confirmed by the relative enrichment of compartment-specific proteins. Contamination of the mitochondrial fraction was assayed by nuclear and cytosolic marker proteins. The mitochondrial Tom40 protein was used to control for enrichment of the mitochondrial fraction. The purity of these mitochondria was highlighted by the fact that they were enriched for Tom40, but not for the abundant nucleo-cytosolic protein PCNA and the cytosolic protein enolase.

Consistent with the literature, etoposide leads to p53 stabilization and accumulation in both the nuclear and mitochondrial compartments of HCT116 cells. In unstressed cells, we detected a low p53 signal in the mitochondrial fraction showing that p53 localized at mitochondria in proliferating conditions. The same observations were obtained with human colorectal carcinoma RKO cells and human fibrosarcoma HT1080 cells (data not shown). The ratio of mitochondrial p53 level to total cellular p53 level is constant between stressed and

unstressed cells and it is of approximately 3% (**Fig. 1A**, right panel). This result suggests that p53 rather accumulate than translocate at mitochondria in stress conditions.

To better define the mitochondrial localization of p53 we next performed subfractionation experiments in unstressed HCT116 cells. First, to test whether p53 was associated with mitochondrial membranes, mitochondria purified from HCT116 cells were alkali-treated and the soluble and membrane fractions were analyzed by immunoblotting (**Fig. 1B**, left panel). p53 is found mostly in the soluble fraction after alkali treatment, but is also weakly detected in the membrane fraction (**Fig. 1B**). As expected, Bak and Tom40, which are embedded in the outer membrane, were recovered only in the pellet fractions while the soluble actin protein (mitochondrial periphery) was found in the supernatant (**Fig. 1B**). Thus, p53 appears not to be embedded in mitochondrial membranes but is soluble and/or weakly associated with membranes. According to these results, p53 could have the following sublocalizations within mitochondria: organelle periphery, intermembrane space and/or matrix.

Next, we performed swelling experiments to disrupt the outer membrane of isolated mitochondria from unstressed HCT116 cells in the presence or absence of proteinase K. **Figure 1C** shows that without osmotic swelling the intermembrane space protein mitofilin and the matrix protein OSCP, a component of the F_1F_0-ATP synthase (complex V of the oxidative phosphorylation chain), are well protected from protease degradation, whereas the extra-mitochondrial protein actin is completely degraded. Quantifications using OSCP as control for both loading and mitochondrial membrane integrity show that p53 is partially degraded (about 50%; **Fig. 1C**, left panel lane 4). Consistent with the literature, this confirms that a fraction of p53 is present at the outer mitochondrial membrane facing the cytosolic compartment. Moreover, proteinase K treatment on mitoplasts highlights a second mitochondrial fraction of p53 that is degraded after protease treatment, as is most of full-length mitofilin (**Fig. 1C**, left panel lane 7). This fraction appears to be located in the

intermembrane space (about 30%). The last mitochondrial fraction of p53 that remains stable and protected from the protease degradation in both intact mitochondria and mitoplasts is therefore located within the mitochondrial matrix (about 20%, **Fig. 1C** lane 7). Altogether our results indicate that p53 can be found in mitochondria in two mitochondrial sub-compartments, i.e. the intermembrane space and matrix, suggesting a multi-functional role for p53.

The H1299-p53-Mx and H1299-p53-IMS stable cell lines respectively express p53 in the mitochondrial matrix and intermembrane space. Since we observed that low levels of endogenous p53 can be located inside mitochondria in unstressed cells, we have constructed a cellular model allowing the study of p53 effects in these specific compartments. We used the H1299 lung carcinoma cell line, which has a homozygous partial deletion of the *TP53* gene and does not express p53, to generate a stable line expressing mitochondrially targeted p53. The stable H1299-p53-Mx cell line results from transfection with a pcDNA3 vector in which the sequence encoding mitochondrial import leader of ornithin transcarbamylase (OTC) was fused to the 5' end of human wild type p53 (**Fig. 2A**, upper left panel). This leader sequence allows the fused protein to be imported inside the mitochondrial matrix where the leader peptide is cleaved off by matrix endopeptidases, and has previously been used to target p53 to mitochondria.[19] A H1299-pcDNA3 control cell line containing the empty vector was also established. An immunoblot of H1299-p53-Mx *versus* pcDNA3 control line confirms low level of p53 expression (**Fig. 2A**, lower left panel). Cellular fractionation and mitochondrial subfractionation were performed to check the intramitochondrial localization of p53 in this cell line. **Figure 2A** (right panel) shows that whole cell lysate (Wcl) contains p53 whereas the fraction containing nuclei and unbroken cells (N*), obtained at the beginning of cellular fractionation, only harbors a small amount of p53. Approximately 5% of cells remained unbroken at this stage, explaining the minor detection of p53 in this fraction as due to contamination by intact cells (data not shown). Compared to Wcl, the fraction enriched in

mitochondria (Ctrl) is highly enriched in p53, indicating that p53 is effectively targeted to mitochondria. Controls of mitochondrial purity and enrichment respectively were tested by nuclear lamins, mitochondrial mitofilin and OSCP, indicating that there is good mitochondrial enrichment and a slight contamination by nuclear components. Interestingly, treatment of the mitochondrial fraction by increasing amounts of proteinase K shows no degradation of p53, indicating that p53 is localized inside mitochondria. The same observation was made with mitoplasts obtained after osmotic choc, demonstrating that p53-Mx is, as expected, localized into the mitochondrial matrix. Indeed, the p53 protein behaves similarly to the matrix OSCP protein, whereas mitofilin, which is inserted into the inner mitochondrial membrane, is mostly degraded. We chose this line since it showed very low basal levels of matrix p53 and did not undergo spontaneous cell death.

The stable H1299-p53-IMS (clone 1, C1) cell line results from transfection with a vector in which the sequence encoding mitochondrial import leader composed of two cleavable sorting signals of cytochrome B2 (CytB2), a soluble protein of the intermembrane space,[60] was fused to the 5' end of human wild type p53 (**Fig. 2B**, upper left panel). A comparison between the H1299-p53-IMS and the pcDNA3 control line confirms that H1299-p53-IMS cells specifically express p53 (**Fig. 2B**, lower left panel). Upon cellular fractionation and mitochondrial subfractionation (**Fig. 2B**, right panel), similar observations than those described for H1299-p53-Mx cells can be made for Wcl, N*, Ctrl fractions and proteinase K treatments on intact mitochondria, indicating that p53-IMS is effectively localized inside mitochondria (actin was used as contamination control instead of lamins). However, proteinase K treatments on mitoplasts shows an almost complete degradation of p53, indicating that p53-IMS is localized in the intermembrane space as expected.

Mitochondrial p53 promotes respiration and decreases ROS production. Mitochondria are the main site of ATP production in cells through oxidative phosphorylation, a process that consumes oxygen but also leads to ROS generation as unavoidable side-product. Recent

evidence indicates that p53 is able to regulate mitochondrial function in unstressed cells through its transcriptional activities. Indeed, p53 activates transcription of nuclear genes coding mitochondrial proteins such as the SCO2, implicated in the cytochrome c oxidase complex assembly of the respiratory chain, or the superoxide dismutase MnSOD that helps detoxifying ROS.[33, 47] Thus, it has been described that p53 increases oxygen consumption rate and diminishes ROS production through its transcriptional functions. Since we and others showed a mitochondrial localization of p53 in unstressed cells, we hypothesized that p53 could also directly regulate mitochondrial bioenergetics in this organelle's physiology. In order to identify mitochondrial functions of p53, we determined whether respiration and ROS production were affected by mitochondrial p53. Oxygen consumption rate and mitochondrial ROS generation rate were measured on HCT116 $p53^{+/+}$ cells compared to HCT116 $p53^{-/-}$ cells (**Fig. 3A**). As previously described in the literature, HCT116 $p53^{+/+}$ cells have higher oxygen consumption and lower mitochondrial ROS than HCT116 $p53^{-/-}$ cells.[33, 61] However, these cells do not permit to discriminate nuclear from direct mitochondrial p53 functions for these activities. To determine whether p53 can directly regulate respiration and ROS production at mitochondria, these two parameters were measured on H1299 pCDNA3, H1299-p53-Mx and H1299-p53-IMS cells. Interestingly, cells with mitochondrial matrix p53 consume significantly more oxygen and produce less mitochondrial ROS than p53 null cells (**Fig. 3B**). Conversely, the oxygen consumption rate of cells with p53 localized in the intermembrane space seems lower than p53 null cells, so p53 localized in this compartment could have an opposite effect compared to p53 localized in the matrix (**Fig. 3C**). In these H1299-p53-IMS cells the mitochondrial ROS generation rate is not modified in comparison to p53 null cells (**Fig. 3C**).

These results suggest that in addition to its related nuclear transcriptional functions, p53 can also directly regulate mitochondrial respiratory activity when localized in the mitochondrial matrix. Apparently, in this internal mitochondrial compartment, p53 promotes respiratory

chain function by mediating an increase in oxygen consumption and a decrease in mitochondrial ROS production. In contrast, p53 localized in the intermembrane space does not seem to regulate this process in the same way. Mitochondrial mass in the three H1299 cell lines was quantified and no detectable difference was found between cells expressing or lacking p53 (data not shown), indicating that p53 does not achieve this effect by increasing mitochondrial mass or numbers per cell but rather appears to fine-tune and optimize the respiratory chain.

p53 interacts with OSCP, a protein of the F_1F_0-ATP synthase. To gain insight into the mechanism of function of mitochondrial matrix p53, we sought to identify p53 partner proteins in mitochondria from unstressed cells. To this end, we used a global approach and performed p53 immunoprecipitation followed by mass spectrometry analysis. p53 immunoprecipitation and negative control immunoprecipitation with irrelevant antibody (normal rabbit IgG) were performed on mitochondria isolated from HCT116 cells untreated or treated with etoposide. The eluted immunoprecipitates were separated by SDS-PAGE before staining with Coomassie blue. The immunoglobulin spots detectable with this staining were removed from gel with a scalpel. The remainder gel containing immunoprecipitated proteins were harvested to analysis. After extraction from gel, proteins were digested with trypsin and the resulting peptides separated by high performance liquid chromatography and analyzed by tandem mass spectrometry.

Three peptides corresponding to the mitochondrial matrix protein Oligomycin Sensitivity-Conferring Protein (OSCP) were identified specifically in p53 immunoprecipitates, but was absent in control IgG immunoprecipitations from etoposide-treated HCT116 cells, suggesting specificity (**Fig. A**). Specifically, OSCP is part of the peripheral stalk of the F_1F_0-ATP synthase, which links the F_0 domain to the F_1 domain and is positioned near the crown region at the top of the F_1 domain.[62] We verified this interaction by

immunoblotting and confirmed that OSCP was weakly but reproducibly detectable in the p53 immunoprecipitate under stressed and unstressed conditions (**Fig. 4B**). In support, a p53-OSCP interaction was also reproducibly detected by p53 immunoprecipitation of purified mitochondria from H1299-p53-Mx cells that express mitochondrial matrix-targeted p53 (**Fig. 4C**). H1299-pcDNA3 cells were used as negative control. Moreover, we used the H1299-p53-IMS clone 2 that expresses mitochondrial p53 at high levels. However, the much higher levels of intermembrane space p53 in H1299-p53-IMS cells interact more weakly with OSCP than the much lower levels of matrix p53 in H1299-p53-Mx cells, consistent with the matrix localization of OSCP protein (**Fig. 4C**). Together, these data demonstrate that OSCP is a novel specific interaction partner of p53 in the matrix of unstressed (and stressed) mitochondria.

The interaction between p53 and OSCP prompted us to investigate the influence of p53 in ATP production, since OSCP is a component of F_1F_0-ATP synthase, the complex which produces ATP from ADP in the presence of a proton gradient generated across the inner membrane by electron transport complexes of the respiratory chain. We measured total and mitochondrial ATP production but observed no difference between cells expressing mitochondrially targeted p53 and $p53^{-/-}$ cells (data not shown). Thus, the interaction of p53 with OSCP does not seem to regulate ATP production but instead might be implicated in ROS regulation by stabilization of oxidative phosphorylation complexes.

OSCP regulates mitochondrial localization of p53. We determined that p53 is able to localize in the mitochondrial matrix in unstressed conditions, with approximately 20% of the total mitochondrial p53 pool present in this compartment (**Fig. 1C**). Thus we next determined if the interaction of p53 with OSCP, a protein located in the matrix, could be implicated in p53 matrix localization. Indeed, p53 does not contain a classical mitochondrial targeting signal and co-transport mechanisms have been proposed for its mitochondrial import.[63] To test this hypothesis, we examined the localization of p53 after knocking down OSCP expression.

HCT116 cells were transfected with siRNA OSCP or nonspecific siRNA as control. Cells were harvested 72 hours after transfection, an aliquot of whole cell lysate was kept and mitochondrial and cytosolic fractions were isolated (**Fig. 5A**). Loading of mitochondrial fractions were normalized to VDAC1 (Voltage Dependent Anion Channel), the most abundant protein of the outer mitochondrial membrane (**Fig. 5B**). We noticed a 70% decrease of OSCP level in mitochondrial fractions of cells treated with siRNA OSCP compared to siRNA control. Interestingly, we observed a 30% reduction of the p53 protein level in the mitochondrial fraction in siOSCP mitochondria compared to control. Conversely, the total amount of cellular p53, normalized to actin levels in total cellular extracts, was not affected by OSCP expression reduction (**Fig. 5C**). These results suggest that OSCP might be implicated in translocation or stability of p53 in the mitochondrial matrix.

p53 is required for F_1F_0-ATP synthase complex assembly or stabilization. To obtain insight into the functional implication of the p53/OSCP interaction apart from mitochondrial localization regulation of p53, we analyzed whether the absence of total or mitochondrial p53 could affect the steady-state level of mature F_1F_0-ATP synthase, using Blue-Native PAGE and immunoblotting. As shown in **Figures 6A** and **6B**, Blue-Native gel immunoblots reveal a decrease of F_1F_0-ATP synthase (20%) in the HCT116 $p53^{-/-}$ cells compared to HCT116 $p53^{+/+}$ cells. In support, F_1F_0-ATP synthase is also reduced (40%) in H1299 pCDNA3 cells compared to H1299-p53-Mx cells (**Figures 6A** and **6C**), while its steady-state level is not significantly different from H1299-p53-IMS cells (**Figures 6A** and **6D**). Hence, contrary to p53-IMS, p53-Mx can directly act on the assembly or stability of F_1F_0-ATP synthase. Interestingly, these results suggest that p53 located in the matrix could affect the organization of one or several oxidative phosphorylation complexes, likely explaining its effects on cell respiration.

Discussion

Until now it was thought that p53 activities which mediate tumor suppression were limited to trigger cell cycle arrest, senescence or apoptosis in stress conditions through transcription-dependent and independent activities. The majority of studies on p53 functions have been performed in stress conditions, where p53 is stabilized at high levels compared to the very low levels of unstressed cells due to high degradative turnover. However, data accumulates indicating an emerging role of p53 at basal levels. p53 notably seems to influence metabolism in the absence of acute stress. Solid data describe that basal p53 can diminish glycolysis, favor oxidative phosphorylation and reduce ROS production by transcription-dependent mechanisms. It has been suggested that these new basal p53 functions could also be important to inhibit tumor development, since metabolic alterations can contribute to cell transformation. Furthermore, several independent studies have shown a mitochondrial localization of p53 in the matrix compartment, where it interacts with DNA polymerase γ and mtTFA, potentially acting on maintenance and fidelity of mtDNA.[64-66]

In this study we identified mitochondrial localization of basal p53 in unstressed cells, using the human wtp53 expressing HCT116 cell line as a model. In the absence of acute stress, the total cellular content of p53 is low and we estimated that approximately 3% of total cellular p53 is localized at mitochondria. Our data indicates that endogenous p53 resides in the intermembrane space and matrix in addition to its outer membrane localization. Furthermore, we observed that p53 is localized in soluble compartments in mitochondria or only weakly bound to mitochondrial membranes, in agreement with the lack of a transmembrane domain prediction within the p53 polypeptide sequence.

p53-dependent transcriptional regulation of several genes encoding mitochondrial proteins implicated in oxidative phosphorylation or ROS scavenging such SCO2, MnSOD and the glutaminase 2 have been previously described.[33, 39, 61] We have hypothesized that p53 can also play a direct role in mitochondrial physiology. To discriminate nuclear from mitochondrial

p53 functions with respect to regulating mitochondrial metabolism, we generated stable cell lines expressing p53 targeted to the mitochondrial intermembrane space or the matrix, the two inner mitochondrial compartments identified as p53 localization sites. We selected cellular clones expressing low mitochondrial p53 levels close to the endogenous levels. This model was used to obtain evidence for new p53 roles at mitochondria. Indeed, p53 localized in the matrix increased oxygen consumption and reduced mitochondrial ROS generation in healthy cells. Conversely, p53 in the intermembrane space does not seem to regulate these processes. Thus, our data indicate that p53 is able to directly regulate mitochondrial oxidative phosphorylation in this organelle, and suggests that this effect occurs in the matrix. These results are consistent with emerging data indicating the regulation of respiration by basal p53 and show that effects observed in HCT116 cells are dependent on both nuclear and mitochondrial p53. It was recently shown that p53 in the matrix activates necrosis cell death after oxidative stress,[67] suggesting that p53 in this compartment can have major activities in the presence or absence of stress.

In our search of how p53 could regulate oxygen consumption and ROS production, we identified the OSCP as a new mitochondrial partner protein of p53 in the matrix compartment. Although this protein is a matrix subunit of F_1F_0-ATP synthase, we found no effect of mitochondrial p53 on ATP production. Instead, this interaction might be involved in mitochondrial p53 import, since we observed that mitochondrial p53 localization is reduced when OSCP expression is knocked down by siRNA. We therefore speculate that OSCP could co-transport p53 in mitochondria or stabilize p53 in the matrix compartment. Indeed, despite intramitochondrial compartment localizations, the p53 polypeptide sequence lacks a mitochondrial-targeting signal, as do an increasing number of nuclear factors that are currently being detected at mitochondria such CREB, NF-κB, or STAT3,[68-70] indicating non-canonical mechanisms of targeting and import. It has already been shown that p53 can be imported into mitochondria by co-transport mechanisms *via* interaction with proteins such as

mtHsp70,[19] Tid1,[71] mitochondrial helicase RECQL4,[63] or OKL38.[72] Furthermore, a very recent study described an import mechanism of the STAT3 nuclear protein into the mitochondrial matrix *via* an interaction with GRIM-19, a subunit of respiratory chain complex I,[73] supporting the fact that such proteins can also be involved in protein transport into mitochondria.

We also provide evidence that matrix p53 takes part in the assembly or stabilization of the mature F_1F_0-ATP synthase complex. Previously a transcriptional effect of p53 on cytochrome c oxidase assembly was described *via* SCO2 induction.[33] Taken together, p53 could act by nuclear and direct mitochondrial functions to promote oxidative phosphorylation.

While our results suggest that p53 localized in the mitochondrial matrix could optimize oxidative phosphorylation by different activities and at different levels: electron transfert chain and F_1F_0-ATP synthase, we have not identified the precise molecular mechanisms of action. To determine if the interaction of p53 with OSCP is involved in this process, interaction domains of these two proteins will need to be determined and interaction mutants established. The mitochondrial respiratory chain complexes assemble into higher-order structures called supercomplexes,[74] which minimize electron leakage during electron transfer between the individual respiratory complexes. These structures therefore prevent ROS generation.[75] p53 might optimize respiratory chain action *via* an indirect mechanism. For example, we speculate that p53 could be involved in the organization of the oxidative phosphorylation complexes and favor efficient cooperation between them, since assembly or steady state levels of the F_1F_0-ATP synthase could influence the organization of others complexes.[76]

Mitochondria are the major site of ROS production. These molecules are important in the redox regulation and in certain signal transductions but an increase in ROS level promotes oxidative stress and causes oxidative damage to nucleic acids, proteins and lipids. Thus,

mitochondrial ROS may contribute to DNA damage and consequently to oncogenic transformation.[77] In addition to nuclear p53, mitochondrial p53 could prevent DNA damage through control of ROS production. Interestingly, some patients suffering from Li-Fraumeni syndrome exhibit an increase of several markers of oxidative stress compared to control.[78] In addition, Sablina et al.[40] have described that p53 depletion prompts an increase in ROS level, and the appearance of DNA mutation. Finally, it was recently reported that knockin mice expressing a p53 mutant (3KR) that is not able to trigger cell-cycle arrest, senescence or apoptosis are still protected from early tumor formation.[79] This p53 3KR mutant is still able to regulate ROS production. In the latter two studies ROS regulation by p53 has been associated with its transcriptional activities.[40, 79] Here we have shown that p53 can also regulate ROS generation directly at mitochondria. In sum, these data strongly suggest that ROS regulation by p53 protects the genome from low oxidative stress, which permanently occurs during normal cell homeostasis and seems to be an intrinsic part of p53's tumor suppressor functions.

Acknowledgments

We thank Dr. Jordi Magrané (*Department of Neurology and Neuroscience, Weill Medical College of Cornell University, New York, NY 10065, USA*) for providing us with the pIRES-cytb2-WTSOD1 plasmid, Dr. Carole H. Sellem (*Université Paris-Sud, Centre de Génétique Moléculaire, UPR3404, CNRS, Gif-sur-Yvette, France*) to have helped us to perform oxygraphy analysis, and Dr. Alain Guillot (*Plate Forme D'Analyse Proteomique de Paris Sud-Ouest INRA, Jouy en Josas, France*) for mass spectrometry analysis.

Disclosure of Potential Conflicts of Interest

No potential conflicts of interest were disclosed.

References

1. Hollstein M, Sidransky D, Vogelstein B, Harris CC. p53 mutations in human cancers. Science 1991; 253:49-53.

2. Fields S, Jang SK. Presence of a potent transcription activating sequence in the p53 protein. Science 1990; 249:1046-9.

3. Raycroft L, Wu HY, Lozano G. Transcriptional activation by wild-type but not transforming mutants of the p53 anti-oncogene. Science 1990; 249:1049-51.

4. Weintraub H, Hauschka S, Tapscott SJ. The MCK enhancer contains a p53 responsive element. Proc Natl Acad Sci U S A 1991; 88:4570-1.

5. el-Deiry WS, Kern SE, Pietenpol JA, Kinzler KW, Vogelstein B. Definition of a consensus binding site for p53. Nat Genet 1992; 1:45-9.

6. Maltzman W, Czyzyk L. UV irradiation stimulates levels of p53 cellular tumor antigen in nontransformed mouse cells. Mol Cell Biol 1984; 4:1689-94.

7. Tishler RB, Calderwood SK, Coleman CN, Price BD. Increases in sequence specific DNA binding by p53 following treatment with chemotherapeutic and DNA damaging agents. Cancer Res 1993; 53:2212-6.

8. Nakamura Y. Isolation of p53-target genes and their functional analysis. Cancer Sci 2004; 95:7-11.

9. Riley T, Sontag E, Chen P, Levine A. Transcriptional control of human p53-regulated genes. Nat Rev Mol Cell Biol 2008; 9:402-12.

10. Wang B, Xiao Z, Ko HL, Ren EC. The p53 response element and transcriptional repression. Cell Cycle 2010; 9:870-9.

11. Zuckerman V, Wolyniec K, Sionov RV, Haupt S, Haupt Y. Tumour suppression by p53: the importance of apoptosis and cellular senescence. J Pathol 2009; 219:3-15.

12. Caelles C, Helmberg A, Karin M. p53-dependent apoptosis in the absence of transcriptional activation of p53-target genes. Nature 1994; 370:220-3.

13. Gottlieb E, Lindner S, Oren M. Relationship of sequence-specific transactivation and p53-regulated apoptosis in interleukin 3-dependent hematopoietic cells. Cell Growth Differ 1996; 7:301-10.

14. Bissonnette N, Wasylyk B, Hunting DJ. The apoptotic and transcriptional transactivation activities of p53 can be dissociated. Biochem Cell Biol 1997; 75:351-8.

15. Yan Y, Shay JW, Wright WE, Mumby MC. Inhibition of protein phosphatase activity induces p53-dependent apoptosis in the absence of p53 transactivation. J Biol Chem 1997; 272:15220-6.

16. Haupt Y, Rowan S, Shaulian E, Vousden KH, Oren M. Induction of apoptosis in HeLa cells by trans-activation-deficient p53. Genes Dev 1995; 9:2170-83.

17. Haupt Y, Rowan S, Shaulian E, Kazaz A, Vousden K, Oren M. p53 mediated apoptosis in HeLa cells: transcription dependent and independent mechanisms. Leukemia 1997; 11 Suppl 3:337-9.

18. Chen X, Ko LJ, Jayaraman L, Prives C. p53 levels, functional domains, and DNA damage determine the extent of the apoptotic response of tumor cells. Genes Dev 1996; 10:2438-51.

19. Marchenko ND, Zaika A, Moll UM. Death signal-induced localization of p53 protein to mitochondria. A potential role in apoptotic signaling. J Biol Chem 2000; 275:16202-12.

20. Mihara M, Erster S, Zaika A, Petrenko O, Chittenden T, Pancoska P, et al. p53 has a direct apoptogenic role at the mitochondria. Mol Cell 2003; 11:577-90.

21. Erster S, Mihara M, Kim RH, Petrenko O, Moll UM. In vivo mitochondrial p53 translocation triggers a rapid first wave of cell death in response to DNA damage that can precede p53 target gene activation. Mol Cell Biol 2004; 24:6728-41.

22. Zhao Y, Chaiswing L, Velez JM, Batinic-Haberle I, Colburn NH, Oberley TD, et al. p53 translocation to mitochondria precedes its nuclear translocation and targets mitochondrial oxidative defense protein-manganese superoxide dismutase. Cancer Res 2005; 65:3745-50.

23. Leu JI, Dumont P, Hafey M, Murphy ME, George DL. Mitochondrial p53 activates Bak and causes disruption of a Bak-Mcl1 complex. Nat Cell Biol 2004; 6:443-50.

24. Chipuk JE, Kuwana T, Bouchier-Hayes L, Droin NM, Newmeyer DD, Schuler M, et al. Direct activation of Bax by p53 mediates mitochondrial membrane permeabilization and apoptosis. Science 2004; 303:1010-4.

25. Deng X, Gao F, Flagg T, Anderson J, May WS. Bcl2's flexible loop domain regulates p53 binding and survival. Mol Cell Biol 2006; 26:4421-34.

26. Vaseva AV, Moll UM. The mitochondrial p53 pathway. Biochim Biophys Acta 2009; 1787:414-20.

27. Sot B, Freund SM, Fersht AR. Comparative biophysical characterization of p53 with the pro-apoptotic BAK and the anti-apoptotic BCL-xL. J Biol Chem 2007; 282:29193-200.

28. Tomita Y, Marchenko N, Erster S, Nemajerova A, Dehner A, Klein C, et al. WT p53, but not tumor-derived mutants, bind to Bcl2 via the DNA binding domain and induce mitochondrial permeabilization. J Biol Chem 2006; 281:8600-6.

29. Petros AM, Gunasekera A, Xu N, Olejniczak ET, Fesik SW. Defining the p53 DNA-binding domain/Bcl-x(L)-binding interface using NMR. FEBS Lett 2004; 559:171-4.
30. Pietsch EC, Perchiniak E, Canutescu AA, Wang G, Dunbrack RL, Murphy ME. Oligomerization of BAK by p53 utilizes conserved residues of the p53 DNA binding domain. J Biol Chem 2008; 283:21294-304.
31. Vousden KH, Prives C. Blinded by the Light: The Growing Complexity of p53. Cell 2009; 137:413-31.
32. Vousden KH, Ryan KM. p53 and metabolism. Nat Rev Cancer 2009; 9:691-700.
33. Matoba S, Kang JG, Patino WD, Wragg A, Boehm M, Gavrilova O, et al. p53 regulates mitochondrial respiration. Science 2006; 312:1650-3.
34. Warburg O. On respiratory impairment in cancer cells. Science 1956; 124:269-70.
35. Schwartzenberg-Bar-Yoseph F, Armoni M, Karnieli E. The tumor suppressor p53 down-regulates glucose transporters GLUT1 and GLUT4 gene expression. Cancer Res 2004; 64:2627-33.
36. Kawauchi K, Araki K, Tobiume K, Tanaka N. p53 regulates glucose metabolism through an IKK-NF-kappaB pathway and inhibits cell transformation. Nat Cell Biol 2008; 10:611-8.
37. Bensaad K, Tsuruta A, Selak MA, Vidal MN, Nakano K, Bartrons R, et al. TIGAR, a p53-inducible regulator of glycolysis and apoptosis. Cell 2006; 126:107-20.
38. Tan M, Li S, Swaroop M, Guan K, Oberley LW, Sun Y. Transcriptional activation of the human glutathione peroxidase promoter by p53. J Biol Chem 1999; 274:12061-6.
39. Hussain SP, Amstad P, He P, Robles A, Lupold S, Kaneko I, et al. p53-induced up-regulation of MnSOD and GPx but not catalase increases oxidative stress and apoptosis. Cancer Res 2004; 64:2350-6.
40. Sablina AA, Budanov AV, Ilyinskaya GV, Agapova LS, Kravchenko JE, Chumakov PM. The antioxidant function of the p53 tumor suppressor. Nat Med 2005; 11:1306-13.
41. O'Connor JC, Wallace DM, O'Brien CJ, Cotter TG. A novel antioxidant function for the tumor-suppressor gene p53 in the retinal ganglion cell. Invest Ophthalmol Vis Sci 2008; 49:4237-44.
42. Velasco-Miguel S, Buckbinder L, Jean P, Gelbert L, Talbott R, Laidlaw J, et al. PA26, a novel target of the p53 tumor suppressor and member of the GADD family of DNA damage and growth arrest inducible genes. Oncogene 1999; 18:127-37.
43. Budanov AV, Shoshani T, Faerman A, Zelin E, Kamer I, Kalinski H, et al. Identification of a novel stress-responsive gene Hi95 involved in regulation of cell viability. Oncogene 2002; 21:6017-31.
44. Polyak K, Xia Y, Zweier JL, Kinzler KW, Vogelstein B. A model for p53-induced apoptosis. Nature 1997; 389:300-5.
45. Rivera A, Maxwell SA. The p53-induced gene-6 (proline oxidase) mediates apoptosis through a calcineurin-dependent pathway. J Biol Chem 2005; 280:29346-54.
46. Liu G, Chen X. The ferredoxin reductase gene is regulated by the p53 family and sensitizes cells to oxidative stress-induced apoptosis. Oncogene 2002; 21:7195-204.
47. Dhar SK, Xu Y, St Clair DK. Nuclear factor kappaB- and specificity protein 1-dependent p53-mediated bi-directional regulation of the human manganese superoxide dismutase gene. J Biol Chem; 285:9835-46.
48. de Souza-Pinto NC, Harris CC, Bohr VA. p53 functions in the incorporation step in DNA base excision repair in mouse liver mitochondria. Oncogene 2004; 23:6559-68.
49. Chen D, Yu Z, Zhu Z, Lopez CD. The p53 pathway promotes efficient mitochondrial DNA base excision repair in colorectal cancer cells. Cancer Res 2006; 66:3485-94.
50. Lebedeva MA, Eaton JS, Shadel GS. Loss of p53 causes mitochondrial DNA depletion and altered mitochondrial reactive oxygen species homeostasis. Biochim Biophys Acta 2009; 1787:328-34.
51. Kulawiec M, Ayyasamy V, Singh KK. p53 regulates mtDNA copy number and mitocheckpoint pathway. J Carcinog 2009; 8:8.
52. Park JY, Wang PY, Matsumoto T, Sung HJ, Ma W, Choi JW, et al. p53 improves aerobic exercise capacity and augments skeletal muscle mitochondrial DNA content. Circ Res 2009; 105:705-12, 11 p following 12.
53. Mahyar-Roemer M, Fritzsche C, Wagner S, Laue M, Roemer K. Mitochondrial p53 levels parallel total p53 levels independent of stress response in human colorectal carcinoma and glioblastoma cells. Oncogene 2004; 23:6226-36.
54. Ferecatu I, Bergeaud M, Rodriguez-Enfedaque A, Le Floch N, Oliver L, Rincheval V, et al. Mitochondrial localization of the low level p53 protein in proliferative cells. Biochem Biophys Res Commun 2009; 387:772-7.
55. De S, Kumari J, Mudgal R, Modi P, Gupta S, Futami K, et al. RECQL4 is essential for the transport of p53 to mitochondria in normal human cells in the absence of exogenous stress. J Cell Sci.
56. Magrane J, Hervias I, Henning MS, Damiano M, Kawamata H, Manfredi G. Mutant SOD1 in neuronal mitochondria causes toxicity and mitochondrial dynamics abnormalities. Hum Mol Genet 2009; 18:4552-64.
57. Bunz F, Dutriaux A, Lengauer C, Waldman T, Zhou S, Brown JP, et al. Requirement for p53 and p21 to sustain G2 arrest after DNA damage. Science 1998; 282:1497-501.

58. Ferecatu I, Le Floch N, Bergeaud M, Rodriguez-Enfedaque A, Rincheval V, Oliver L, et al. Evidence for a mitochondrial localization of the retinoblastoma protein. BMC Cell Biol 2009; 10:50.
59. Burden DA, Osheroff N. Mechanism of action of eukaryotic topoisomerase II and drugs targeted to the enzyme. Biochim Biophys Acta 1998; 1400:139-54.
60. Ono H, Gruhler A, Stuart RA, Guiard B, Schwarz E, Neupert W. Sorting of cytochrome b2 to the intermembrane space of mitochondria. Kinetic analysis of intermediates demonstrates passage through the matrix. J Biol Chem 1995; 270:16932-8.
61. Hu W, Zhang C, Wu R, Sun Y, Levine A, Feng Z. Glutaminase 2, a novel p53 target gene regulating energy metabolism and antioxidant function. Proc Natl Acad Sci U S A 2010; 107:7455-60.
62. Rubinstein J, Walker J. ATP synthase from Saccharomyces cerevisiae: location of the OSCP subunit in the peripheral stalk region. J Mol Biol 2002; 321:613-9.
63. De S, Kumari J, Mudgal R, Modi P, Gupta S, Futami K, et al. RECQL4 is essential for the transport of p53 to mitochondria in normal human cells in the absence of exogenous stress. J Cell Sci 2012; 125:2509-22.
64. Yoshida Y, Izumi H, Torigoe T, Ishiguchi H, Itoh H, Kang D, et al. P53 physically interacts with mitochondrial transcription factor A and differentially regulates binding to damaged DNA. Cancer Res 2003; 63:3729-34.
65. Achanta G, Sasaki R, Feng L, Carew JS, Lu W, Pelicano H, et al. Novel role of p53 in maintaining mitochondrial genetic stability through interaction with DNA Pol gamma. EMBO J 2005; 24:3482-92.
66. Bakhanashvili M, Grinberg S, Bonda E, Rahav G. Excision of nucleoside analogs in mitochondria by p53 protein. AIDS 2009; 23:779-88.
67. Vaseva AV, Marchenko ND, Ji K, Tsirka SE, Holzmann S, Moll UM. p53 opens the mitochondrial permeability transition pore to trigger necrosis. Cell 2012; 149:1536-48.
68. Lee J, Kim CH, Simon DK, Aminova LR, Andreyev AY, Kushnareva YE, et al. Mitochondrial cyclic AMP response element-binding protein (CREB) mediates mitochondrial gene expression and neuronal survival. J Biol Chem 2005; 280:40398-401.
69. Cogswell PC, Kashatus DF, Keifer JA, Guttridge DC, Reuther JY, Bristow C, et al. NF-kappa B and I kappa B alpha are found in the mitochondria. Evidence for regulation of mitochondrial gene expression by NF-kappa B. J Biol Chem 2003; 278:2963-8.
70. Wegrzyn J, Potla R, Chwae YJ, Sepuri NB, Zhang Q, Koeck T, et al. Function of mitochondrial Stat3 in cellular respiration. Science 2009; 323:793-7.
71. Ahn BY, Trinh DL, Zajchowski LD, Lee B, Elwi AN, Kim SW. Tid1 is a new regulator of p53 mitochondrial translocation and apoptosis in cancer. Oncogene 2010; 29:1155-66.
72. Hu J, Yao H, Gan F, Tokarski A, Wang Y. Interaction of OKL38 and p53 in regulating mitochondrial structure and function. PLoS One 2012; 7:e43362.
73. Tammineni P, Anugula C, Mohammed F, Anjaneyulu M, Larner AC, Sepuri NB. The import of the transcription factor STAT3 into mitochondria depends on GRIM-19, a component of the electron transport chain. J Biol Chem 2013; 288:4723-32.
74. Schagger H, Pfeiffer K. Supercomplexes in the respiratory chains of yeast and mammalian mitochondria. EMBO J 2000; 19:1777-83.
75. Lenaz G, Baracca A, Barbero G, Bergamini C, Dalmonte ME, Del Sole M, et al. Mitochondrial respiratory chain super-complex I-III in physiology and pathology. Biochim Biophys Acta 2010; 1797:633-40.
76. Wittig I, Schagger H. Supramolecular organization of ATP synthase and respiratory chain in mitochondrial membranes. Biochim Biophys Acta 2009; 1787:672-80.
77. Martindale JL, Holbrook NJ. Cellular response to oxidative stress: signaling for suicide and survival. J Cell Physiol 2002; 192:1-15.
78. Macedo GS, Lisboa da Motta L, Giacomazzi J, Netto CB, Manfredini V, Vanzin CS, et al. Increased oxidative damage in carriers of the germline TP53 p.R337H mutation. PLoS One 2012; 7:e47010.
79. Li T, Kon N, Jiang L, Tan M, Ludwig T, Zhao Y, et al. Tumor suppression in the absence of p53-mediated cell-cycle arrest, apoptosis, and senescence. Cell 2012; 149:1269-83.

Figure Legends

Figure 1. Endogenous p53 resides in different mitochondrial compartments in unstressed cells.

(**A**) Left panel: 15 µg of whole cell lysates (Wcl), nuclei plus unbroken cells (N*), cytosolic fraction (Cy), and mitochondrial fraction (M) of HCT116 cells treated or untreated with 125µg/ml of etoposide for 24 hours were subjected to immunoblot analysis for p53, PCNA, Enolase and Tom40. Right panel: Densitometry of blot in the left panel. The ratio of mitochondrial p53 /total cellular p53 levels was calculated to determine the relative amount of the mitochondrial p53. (**B**) Left panel: 300 µg of mitochondrial protein isolated from HCT116 cells were treated with sodium carbonate (pH 11.5) and ultracentrifuged. The soluble proteins were recovered in the supernatant (S), while the integral membrane proteins remained in the pellet (P). Proteins were subjected to immunoblot analysis for p53, PCNA, actin, Bak and Tom40. Right panel: The level of p53, actin, Tom40 and Bak proteins was quantified in soluble and membrane fractions after alkali treatment by densitometry of blot in the left panel. (**C**) Left panel: 50 µg of mitochondrial proteins isolated from mitochondria of unstressed HCT116 cells were treated with increasing quantities of proteinase K (K; 150 ng, 300 ng and 450 ng) prior to (mitochondria, lanes 2-4) or after swelling (mitoplasts, lanes 5-7). Swelling disrupts the outer membrane while keeping the inner membrane intact. Untreated mitochondrial extracts were used as control (Ctrl). Samples were subjected to immunoblot analysis for p53 and marker proteins of different mitochondrial subcompartments: OSCP (matrix), mitofilin (IMS), actin (mitochondrial periphery). Right panel: Densitometry of blot in the left panel. The mitochondrial matrix protein OSCP was used as control for loading and mitochondrial membrane integrity. The levels of p53, actin and mitofilin were normalized to OSCP in each condition (lanes 1, 4, 7) and compared with intact mitochondria (M) or mitoplasts (Mitopl) treated or not treated (Ctrl) with proteinase K (K).

Figure 2. Targeting of p53 to the mitochondrial matrix and intermembrane space in H1299 cells.

(**A**) Characterization of the stable H1299-p53-Mx cell line. Left upper panel: Schematic representation of the cDNA construct to target p53 to the mitochondrial matrix (p53-Mx): the mitochondrial import leader of ornithin transcarbamylase (OTC) is fused to human wild type p53 in pcDNA3 expression vector. Left lower panel: Low level expression of p53-Mx was assessed by immunoblot of whole cell lysates of H1299-p53-Mx *versus* H1299 pcDNA3 control line. Actin served as a loading control. Right panel: Mitochondrial purification and subfractionation. 15 μg of all fractions: whole cell lystates (Wcl), nuclei plus unbroken cells (N*), mitochondria and mitoplasts treated with increasing concentrations of proteinase K (K), or left untreated (Ctrl) of H1299-p53-Mx cells were loaded on the same gel. The blot was subjected to immunoblot analysis with anti-p53, anti-lamins, anti-mitofilin and anti-OSCP antibodies. (**B**) Characterization of the stable H1299-p53-IMS clone (C1) cell line. Left upper panel: Schematic representation of the cDNA construct to target p53 to the intermembrane space (p53-IMS): mitochondrial import leader of cytochrome B2 (CytB2), composed of two cleavable sorting signals, fused to human wild type p53. Left lower panel: Expression of p53-IMS was assessed by immunoblot on the H1299-p53-IMS C1 *versus* the H1299 pcDNA3 control line. Right panel: The same treatments and immunoblot were performed as for H1299-p53-Mx cells.

Figure 3. Mitochondrial matrix p53 promotes oxygen consumption and decreases ROS production.

Average values of oxygen consumption rate and mitochondrial ROS generation in unstressed (**A**) HCT116 $p53^{+/+}$ *versus* HCT116 $p53^{-/-}$ cells, (**B**) H1299-p53-Mx *versus* H1299 pcDNA3 cells, (**C**) H1299-p53-IMS *versus* H1299 pcDNA3 cells. Oxygen consumption was measured with a Clark electrode. Mitochondrial superoxide anion level was determined with the MitoSOX probe.

Figure 4. p53 interacts with the OSCP subunit of the F_1F_0-ATP synthase complex of mitochondria.

(**A**) Extracts from isolated mitochondria from HCT116 cells, untreated or treated with etoposide for 24 hours, were immunoprecipitated with p53 antibodies (FL393) or control antibody (IgG). p53 and control immunoprecipitations were subjected to mass spectrometry analysis. Three peptides were specifically identified in p53 immunoprecipitations under stress conditions (upper panel). These peptides (bold underlined) correspond to the OSCP protein sequence. (**B**) The same immunoprecipitations (IP) and mitochondrial extracts (Input) were loaded on the same gel and analyzed by immunoblot using antibodies to p53 (DO1) and OSCP. Tom40 serves as negative control. (**C**) Mitochondrial extracts from H1299 p53-Mx, p53-IMS and pcDNA3 as control were immunoprecipitated with p53 antibodies (FL393) or not (Input), loaded on the same gel and analyzed by immunoblot using antibodies to p53 (DO1) and OSCP, and MnSOD as negative control.

Figure 5. Knockdown of OSCP results in a decrease of mitochondrial p53 levels.

HCT116 $p53^{+/+}$ cells were transfected with OSCP siRNA or control siRNA (Ctrl). After 72 hours cells were harvested, and whole cell extracts (Wcl), cytosol (Cy) and mitochondrial (M) fractions were prepared and loaded on the same gel. (**A**) Immunoblot analysis. Membrane was probed for OSCP, p53, VDAC1 and actin. These latter two proteins were used as loading control of mitochondria and total cellular extracts, respectively. (**B**, **C**) Densitometry of blot in A. (**B**) OSCP and p53 levels in mitochondrial fraction were normalized to their respective VDAC1 levels. (**C**) OSCP and p53 levels in total cellular extract were normalized to their respective actin levels in knockdown and Ctrl condition.

Figure 6. Mitochondrial p53 increases mature F_1F_0-ATP synthase steady state levels. Mitochondrial proteins isolated from isogenic HCT116 (+/- endogenous wtp53) and H1299

cells (+/- matrix or IMS p53) were solubilized with 1% digitonin, analyzed by BN-PAGE and immunoblotted for OSCP and Tom40. Under the conditions employed, an antibody to OSCP recognizes the F_1F_0-ATP synthase holoenzyme (at approximately 600kDa probably in dimeric form) and no individual F1-ATP synthase subcomplexes. The TOM complex detected by anti-Tom40 antibody runs at 440 kDa and served as loading control of mitochondrial protein complexes. (**A**) Example of BN-PAGE immunoblotting. (**B**, **C**, **D**) Densitometry of BN-PAGE blots. Quantification of F_1F_0-ATP synthase level was normalized to Tom40 in (**B**) HCT116 $p53^{+/+}$ *versus* HCT116 $p53^{-/-}$ cells, in (**C**) H1299-p53-Mx *versus* H1299 pcDNA3 cells, in (**D**) H1299-p53-IMS *versus* H1299-pcDNA3 cells.

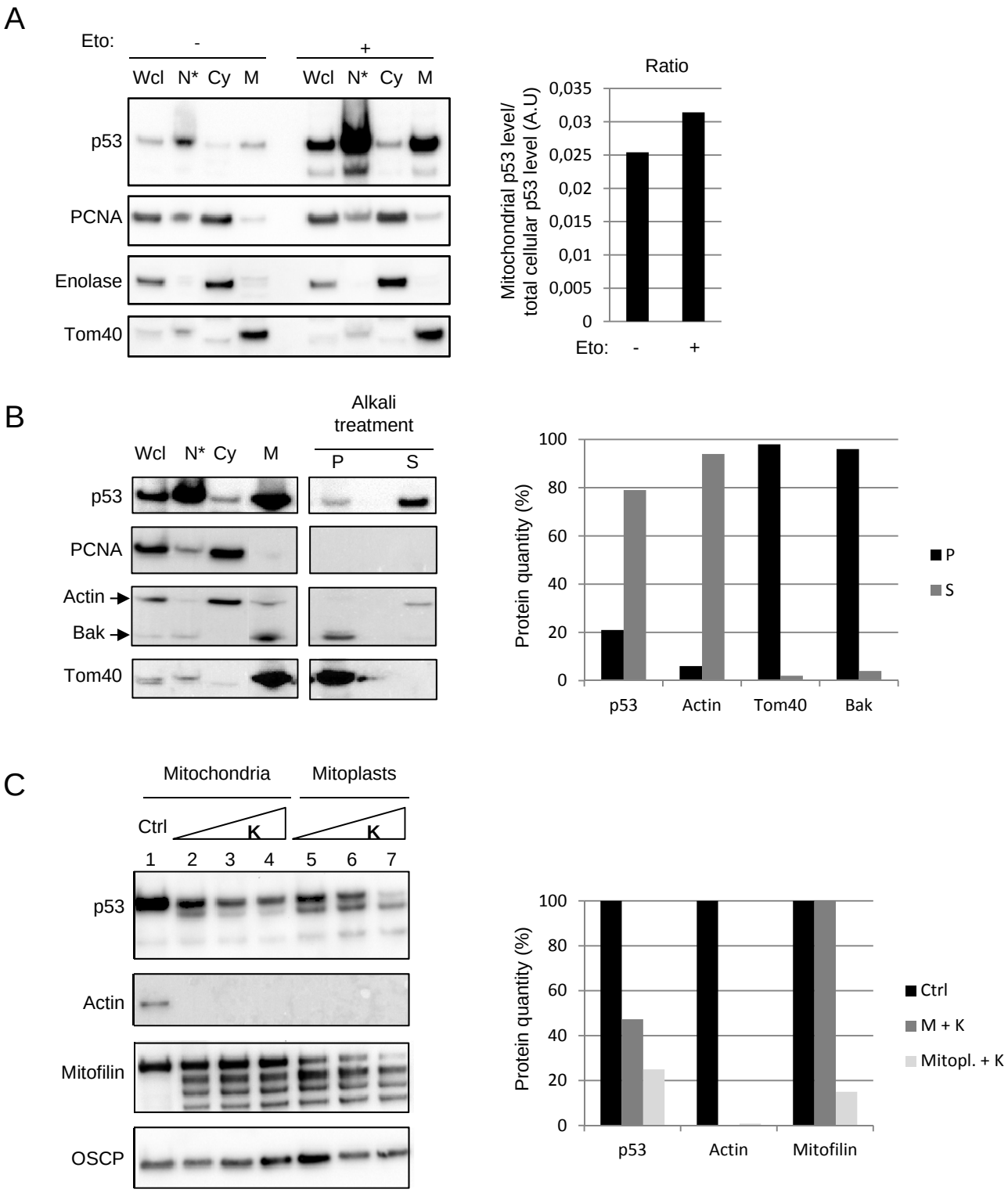
A
Eto:
-
+
Wcl N* Cy M
Wcl N* Cy M
p53
PCNA
Enolase
Tom40
Ratio
Mitochondrial p53 level/
total cellular p53 level (A.U)
0,035
0,03
0,025
0,02
0,015
0,01
0,005
0
Eto: - +
B
Alkali
treatment
Wcl N* Cy M
P S
p53
PCNA
Actin
Bak
Tom40
Protein quantity (%)
100
80
60
40
20
0
p53 Actin Tom40 Bak
P
S
C
Mitochondria
Mitoplasts
Ctrl
K
K
1 2 3 4 5 6 7
p53
Actin
Mitofilin
OSCP
Protein quantity (%)
100
80
60
40
20
0
p53 Actin Mitofilin
Ctrl
M + K
Mitopl. + K

Figure 1

A

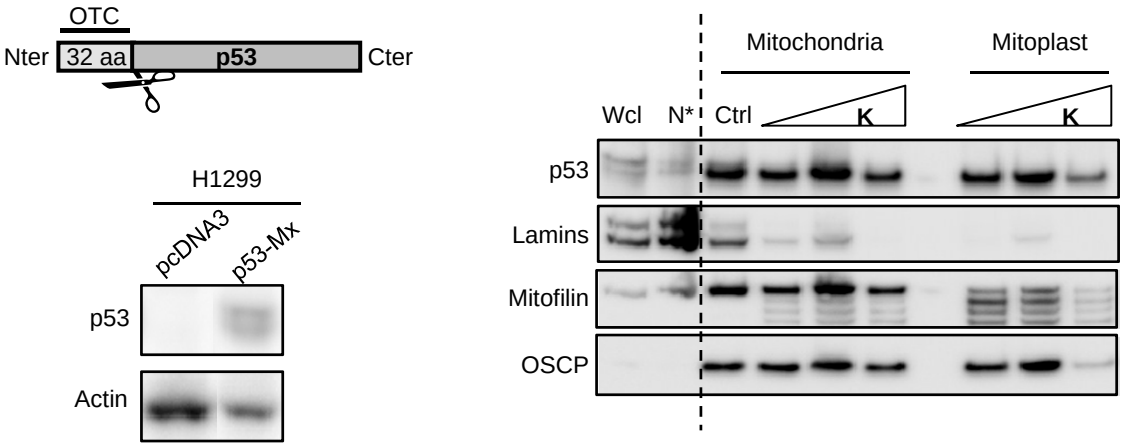
OTC
Nter
32 aa
p53
Cter
H1299
pcDNA3
p53-Mx
p53
Actin
Mitochondria
Mitoplast
Wcl
N*
Ctrl
K
K
p53
Lamins
Mitofilin
OSCP

B

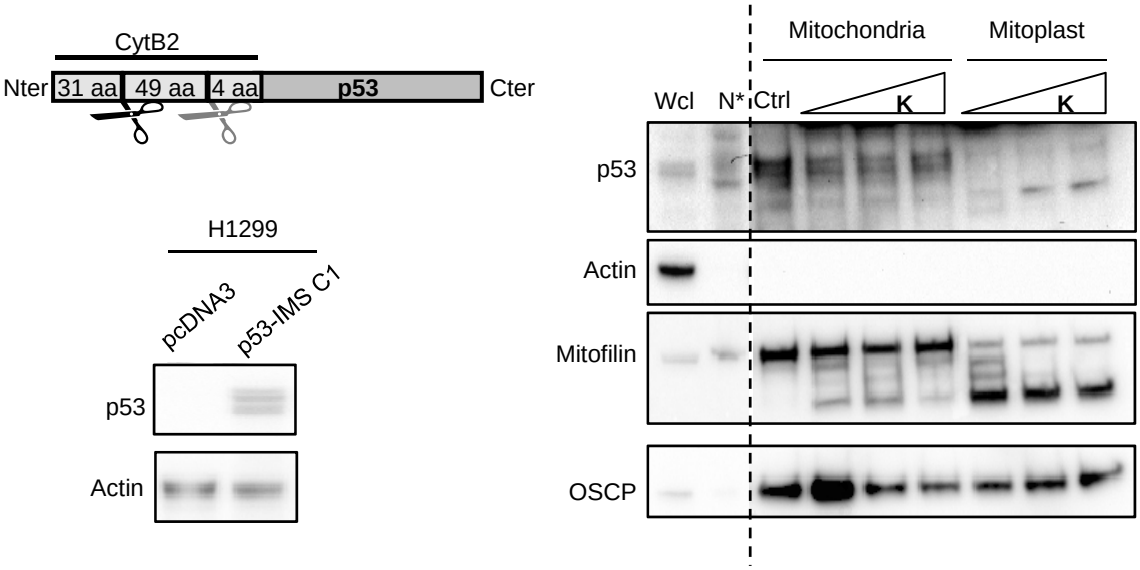
CytB2
Nter
31 aa
49 aa
4 aa
p53
Cter
H1299
pcDNA3
p53-IMS C1
p53
Actin
Mitochondria
Mitoplast
Wcl
N*
Ctrl
K
K
p53
Actin
Mitofilin
OSCP

Figure 2

A

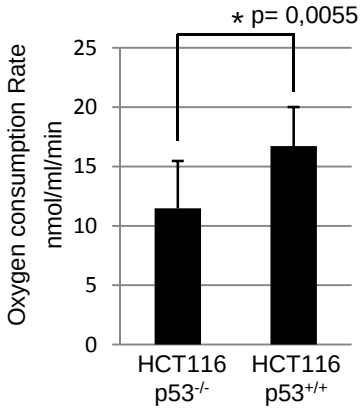
* p= 0,0055
Oxygen consumption Rate
nmol/ml/min
25
20
15
10
5
0
HCT116 p53-/-
HCT116 p53+/+

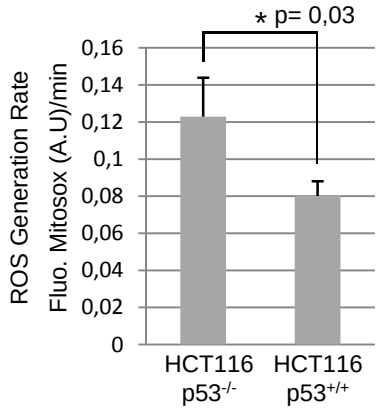
* p= 0,03
ROS Generation Rate
Fluo. Mitosox (A.U)/min
0,16
0,14
0,12
0,1
0,08
0,06
0,04
0,02
0
HCT116 p53-/-
HCT116 p53+/+

B

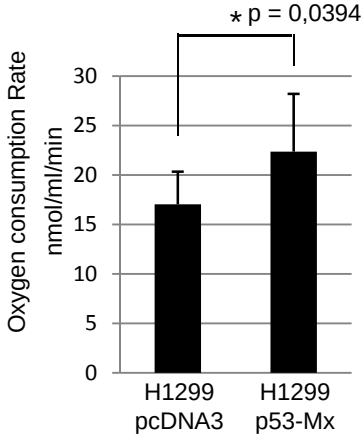
* p = 0,0394
Oxygen consumption Rate
nmol/ml/min
30
25
20
15
10
5
0
H1299 pcDNA3
H1299 p53-Mx

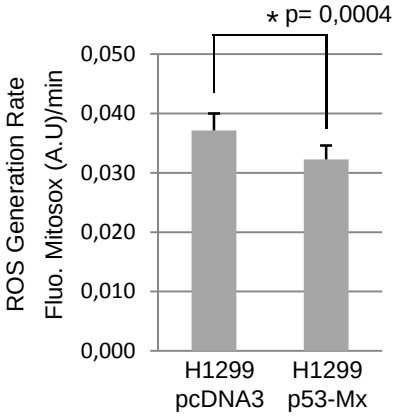
* p= 0,0004
ROS Generation Rate
Fluo. Mitosox (A.U)/min
0,050
0,040
0,030
0,020
0,010
0,000
H1299 pcDNA3
H1299 p53-Mx

C

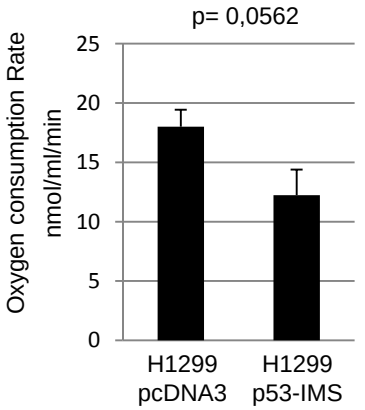
p= 0,0562
Oxygen consumption Rate
nmol/ml/min
25
20
15
10
5
0
H1299 pcDNA3
H1299 p53-IMS

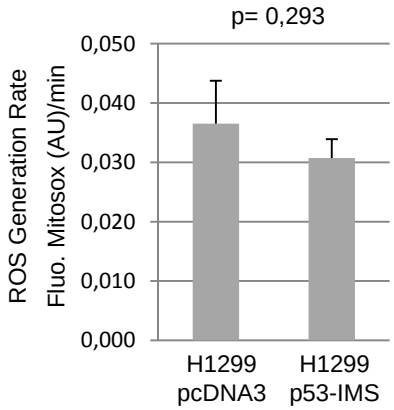
p= 0,293
ROS Generation Rate
Fluo. Mitosox (AU)/min
0,050
0,040
0,030
0,020
0,010
0,000
H1299 pcDNA3
H1299 p53-IMS

Figure 3

A

*VAASVLNPYVK
*SFLSQGQVLK
*LVRPPVQVYGIEGR

10 20 30 40 50
MAAPAVSGLS RQVRCFSTSV VRPFAK**LVRP** **PVQVYGIEGR** YATALYSAAS
60 70 80 90 100
KQNKLEQVEK ELLRVAQILK **EPKVAASVLN** **PYVK**RSIKVK SLNDITAKER
110 120 130 140 150
FSPLTTNLIN LLAENGRLSN TQGVVSAFST MMSVHRGEVP CTVTSASPLE
160 170 180 190 200
EATLSELKTV LK**SFLSQGQV** **LK**LEAKTDPS ILGGMIVRIG EKYVDMSVKT
210
KIQKLGRAMR EIV

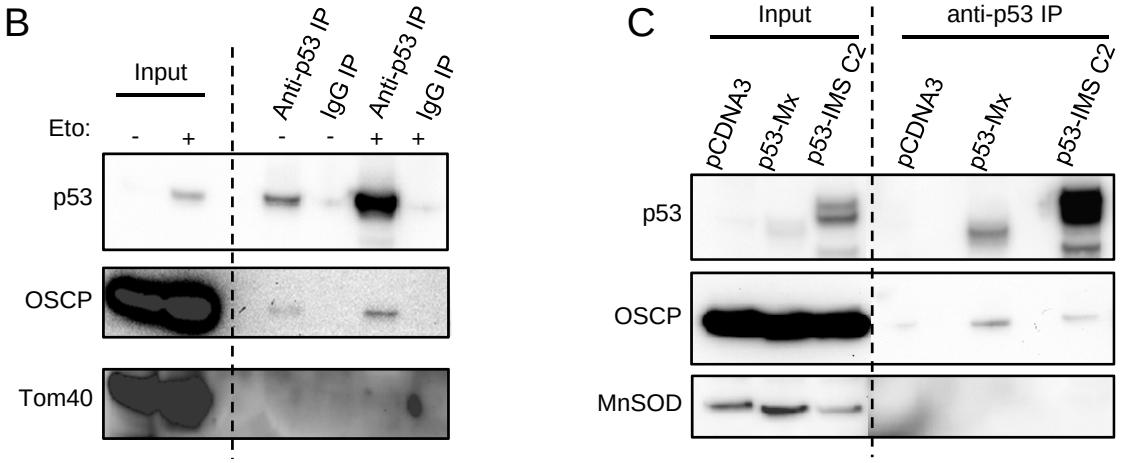

Figure 4

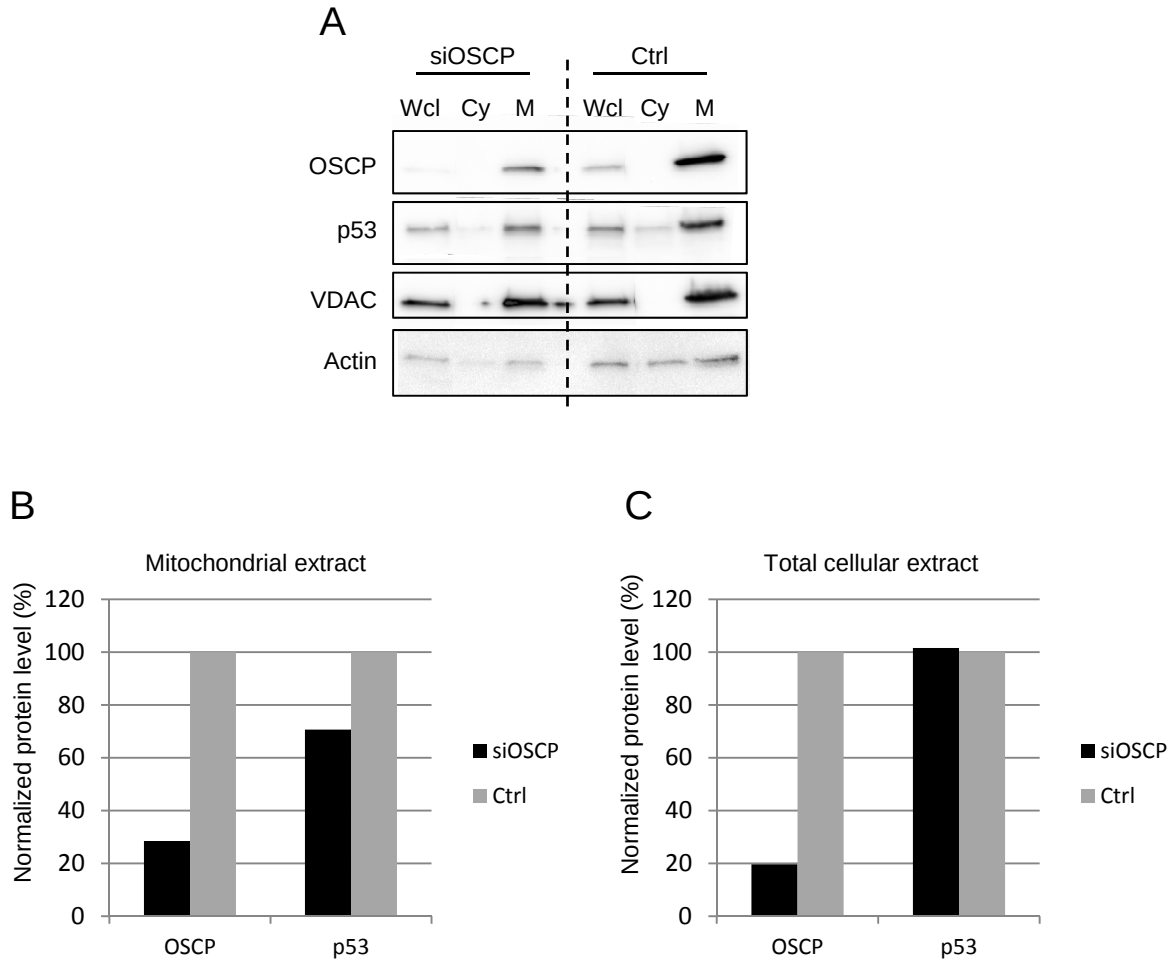
A
siOSCP
Ctrl
Wcl Cy M Wcl Cy M
OSCP
p53
VDAC
Actin
B
Mitochondrial extract
Normalized protein level (%)
120
100
80
60
40
20
0
OSCP
p53
siOSCP
Ctrl
C
Total cellular extract
Normalized protein level (%)
120
100
80
60
40
20
0
OSCP
p53
siOSCP
Ctrl

Figure 5

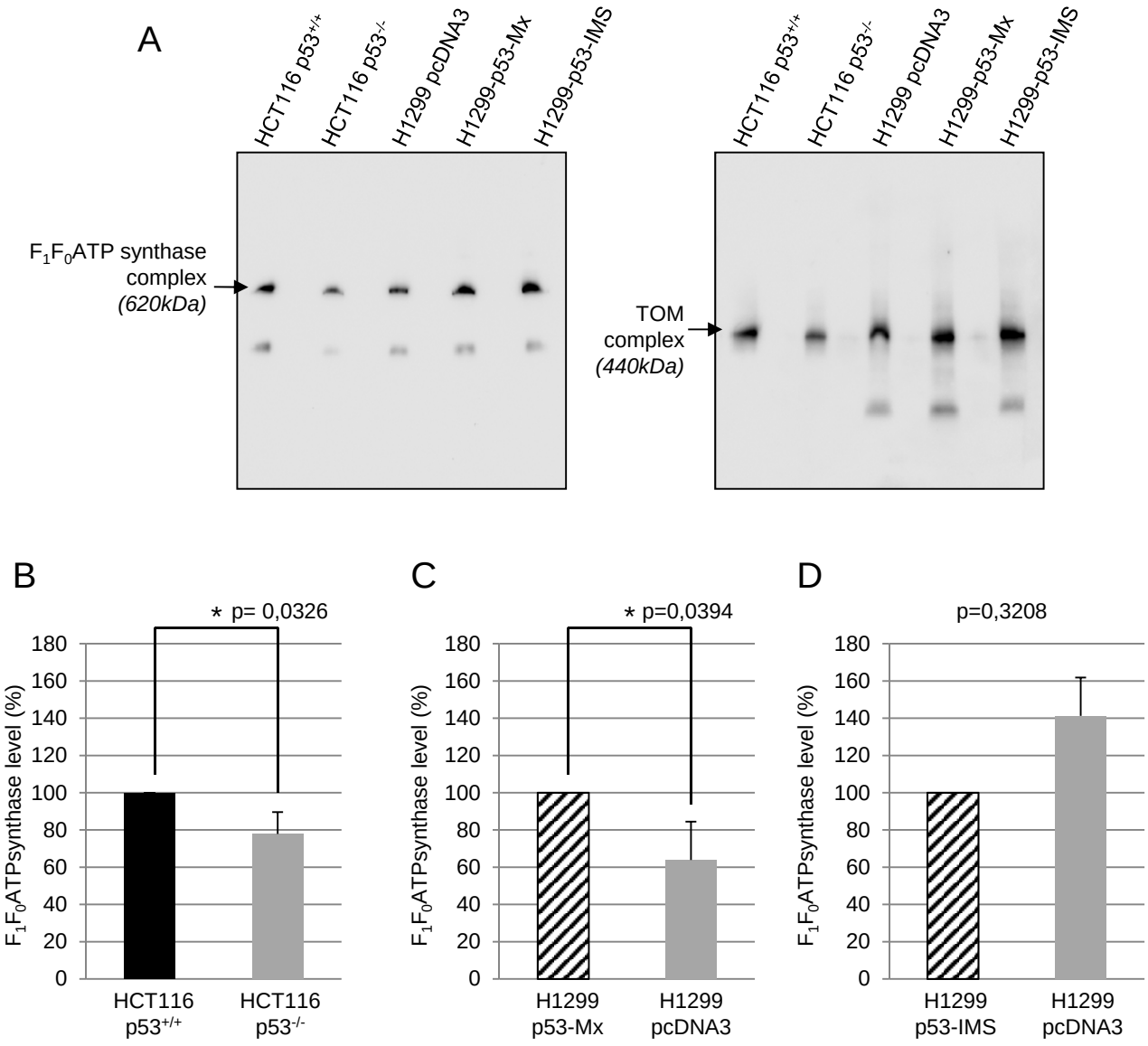
A
HCT116 p53+/+
HCT116 p53-/-
H1299 pcDNA3
H1299-p53-Mx
H1299-p53-IMS
F1F0ATP synthase complex (620kDa)
TOM complex (440kDa)
B
* p= 0,0326
F1F0ATPsynthase level (%)
HCT116 p53+/+
HCT116 p53-/-
C
* p=0,0394
H1299 p53-Mx
H1299 pcDNA3
D
p=0,3208
H1299 p53-IMS
H1299 pcDNA3

Figure 6